Modeling Patagonian ice sheet extent during past glaciations

Nat Wilson

Mark T. Brandon and Ronald B. Smith

April 28, 2009

Abstract:

The circa 20 ka Last Glacial Maximum and the circa 1 Ma Greatest Patagonian Glaciation are noteworthy events in the glacial chronology of the Southern Andes. These glacial advances are thought to be responses to shifts in the balance of glacier accumulation and ablation, in which the glacier equilibrium line moves to lower elevations. This related to changing climatic conditions. The goal of this project is to investigate the nature of these climatic variations and to determine their relative importance in driving a glaciation in the Andes. A glacier flow-routing model solved on a finite difference grid is combined with an orographic precipitation algorithm to simulate the growth and retreat of the Northern Patagonian Ice Field over time scales of tens of thousands of years. This differs from previous explorations of the subject with the mass balance term treating accumulation and ablation separately, where accumulation involves orographic effects, storm frequency, and atmospheric conditions. Ablation is a function of topography and season. As a result, an equilibrium mass balance line is generated based on physical parameters. To ensure the validity of the model, the portion of the LGM ice sheet in the vicinity of Lago Buenos Aires has been simulated and compared to other models and ice sheet proxies. Attempts to recreate a GPG ice sheet primarily by increasing precipitation were unsuccessful, suggesting that an ice cap extending to the farthest mapped moraines must be forced in part by a large temperature depression, in addition to high precipitation delivery.

Introduction:

The purpose of this thesis is to explore the glacial record of the Lago Buenos Aires region in northern Patagonia by means of an ice flow-routing model coupled to accumulation and ablation algorithms. The glacial histories of regions around the world are directly applicable to better understanding large-scale climate cycles. Investigating the glacial record and the swings in climate that it implies is important for developing a better awareness of our modern climate (Hartmann, 1994).

The increase in available computational power in recent decades has improved the scale and complexity feasible within glacial modeling. Several groups have used these models to investigate glaciation within the Andes. Some early models have used coarse spatial grids in order to predict the general characteristics of entire Andean ice caps during a glacial period (Hulton et al., 1994, 2002). Others have focused on smaller regions with finer spatial scales that permit the spontaneous generation

A senior thesis presented to the faculty of the Department of Geology and Geophysics, Yale University,
in partial fulfillment of the Bachelor's Degree.

of individual streams of ice through larger valleys within the mountain range (Hubbard et al., 2005). Some groups have found ice cap modeling to be applicable in exploring the role of glacial erosion on topography (Herman and Braun, 2008; Kaplan et al., 2009). Whereas most of these models have had simple mass balance terms intended approximate the observed and inferred snow lines and mass fluxes, we apply a mass balance that separates accumulation and ablation into independent calculations. The spatial accumulation distribution is based on a linear theory of orographic precipitation (Smith and Barstad, 2004), whereas ablation is based on a degree-day factor, calculated with concern for season. Using this approach, we investigate climatic parameters (temperature and storm frequency) needed to induce a glaciation with more control over the questions asked. The ability to separate ablation and accumulation and generate an ELA from scratch allows us to test the hypothesis that major glaciations can be induced by large changes in mass delivery, without major temperature depressions. Northward shifts in the westerlies have been suggested as a cause of southern hemisphere glaciation (Douglass et al., 2005). The high resolution and detail of glacial deposit mapping in the vicinity of Lago Buenos Aires allows us to test this hypothesis and compare model solutions with field observations.

Region of Study:

The Northern Patagonian ice cap, extending in the modern from about 46.5ºS south to 47.5ºS latitude, is well suited for modeling experiments for several reasons. The high topography of the Andes and large supply of moisture from the Pacific Ocean permit the development of large continental glaciers. The latitude of the ice sheet places it in the path of consistent westerly mid-latitude winds (Smith and Evans, 2006; Trenberth, 1991), which makes it easier to predict a distribution of incoming precipitation compared to a region with more ephemeral or complicated wind patterns. The Lago Buenos Aires region to the east, into which the ice sheet has extended in the past, preserves a rich record of moraines and glacially-processed till deposits from multiple glacial advances. Despite these advantages, a significant disadvantage of the field area is the unavailability of modern climate data. Several interpolated and reanalysis data sets exist, however, which provide guidance in interpreting the modern annual and monthly climate conditions.

The glacial moraines, which curl around the shoreline of Lago Buenos Aires on the Argentinian side of the Chilean-Argentine border, are perhaps one of the best sources of data from the region. They consist of broadly curvilinear features composed of poorly sorted silts, cobbles, and boulders transported from within the Andes. A wide variety of rock types are seen within these features, including metamorphic and both intrusive and extrusive igneous rocks (Kaplan et al., 2004), suggesting a wide provenance. A broad source area for the sediments that comprise the features is consistent with an interpretation of deposition by a large ice sheet (figure 1). Because of the dry lee-slope climate of eastern Patagonia, preservation of moraines and other evidence of glaciations such as tills is favored. The locations of the moraines provide information that can be used from a modeling perspective the scale the calculated ice extent to the available record. The moraines are divided into informal groups, based on the distance from the range to the west. By combining the mapped moraine extents with knowledge of the chronology of their deposition, one can employ them as benchmarks for referencing a modeled ice sheet.

The chronology of ice advances has been explored using a variety of methods, including $^{40}Ar/^{39}Ar$ dating of nearby flood basalts (Singer, 2004; Mercer, 1983) and cosmogenic radionuclide dating of exposed boulders (Kaplan et al., 2004). Taken together, previous studies grant a reasonably clear picture of the sequence of preserved regional glaciations (figure 2). The Menucos and Fenix series of moraines date from the Last Glacial Maximum (LGM), and have exposure ages less than 23 ka (Kaplan et al., 2004; Douglas et al., 2006). A series of older glaciations deposited the Moreno, Deseado, and Telken sets of moraines further to the west. The Telken VII moraine is too old and weathered to be dated using cosmogenic nuclide exposure methods; however, its age has been bracketed to 1 Ma using $^{40}Ar/^{39}Ar$ dating of underlying and overlying basalts (Singer, 2004). The glaciation with extent great enough to deposit this moraine has been referred to as the Greatest Patagonian Glaciation (GPG).

Several groups have investigated evidence of the magnitude of the climatic changes needed to drive these glaciations. By comparing what is known of the glacial chronology with pollen records, Denton et al. estimate that an LGM glaciation would have been accompanied by a temperature depression of 6-8º Celsius compared to modern values (1999). This has been corroborated by at least one range-scale glacier model, which found that a depression equivalent to 6º at sea level created an ice cap over the Andes of a

scale similar to the LGM (Hulton et al., 2002). The change in temperature can be roughly converted to a change in equilibrium line altitude (ELA), which is the elevation at which net accumulation over a water year is matched by ablation over the same period. The dependence of ELA on temperature depends on seasonality and lapse rate.

Methods:

Topographical input

The topography is represented by a DEM derived from the Shuttle Radar Topography Mission (SRTM), covering the space between 46ºS-47.3ºS and 74ºW-70.3ºW. This domain extends just beyond the extent of the continental shelf on the weather side of the range, and about 70 km east of the current shoreline of Lago Buenos Aires on the lee side. This area also encloses both the prominent Fenix (LGM) and more eroded Telken VII (GPG) moraines. The approximately 225 km north-south extent of the domain is chosen to avoid allowing edge effects to significantly influence the region of primary interest. The topographic grid-spacing of 925 m allows medium-sized valleys to be resolved, in contrast to previous efforts to model the area that used grid-spacing from 2 km (Hubbard, et al., 2005) to 20 km (Hulton, et al., 1994).

Because the SRTM-derived DEM does not include inland bathymetric data, water-covered areas such as lakes and channels appear as flat surfaces, with an elevation corresponding to the water level. Although small amounts of ice would float, large glacier tongues of the thicknesses being considered would contact the present lake bed. In order to simulate the movement of a very large ice sheet, the Lago Buenos Aires lake bottom needs built into the DEM. To approximate a dry lake bed, first the modern lake and shore line are identified, and used to create a topographical mask (figure 3). The topography outside of this mask is retained as a boundary condition. In the space within this mask, point measurements of bathymetry (Murdie, et al., 1999) are combined into a longitudinal depth profile along the lake. The domain is then re-gridded using a cubic interpolation scheme to recreate the “dry” topography.

The DEM adds the present ice thickness onto the bedrock, which presents a problem because the bedrock topography below the current ice is not well enough known to justify removing the ice cap in a

way similar to how the lake is emptied. The thickness of the present ice cap is not inconsequential, with gravity-based estimates yielding a mean thickness on the order of 1 km (Casassa, 1986). Others have responded to this problem by arguing that the current ice extent is a small fraction of the glacial period extents, and leaving the ice in place (Hubbard et al., 2005). This is repeated here, with the advisory that neglecting the modern ice will alter the rate at which ice flows from the higher parts of the ice cap.

Ice flow

Glacier flow routing is accomplished using an adaptation of the established ICE program, which has been employed in the Southern Alps of New Zealand (Herman and Braun, 2008). The changing mass of a column of ice is the net inflow and outflow, plus a vertical mass balance term.

$$\frac{\delta h}{\delta t} = \bigtriangledown(hu) + M$$

Here, *h* is the thickness of the ice sheet in any given grid cell, and *u* the vertically averaged ice velocity vector. The *M* term refers to accumulation and ablation.

The velocity, *u*, is treated within ICE to be the sum of internal ice sheet deformation and basal sliding. ICE models the movement of ice columns based on a power-law ice rheology. The two components, u_d and u_s, are described as

$$u_d = \frac{2B}{p+2}(\rho g)^p h^{p+1} \left|\bigtriangledown (h+z)\right|^{p-1} \bigtriangledown (h+z)$$

$$u_s = \frac{B_s}{N-P}(\rho g)^p h^p \left|\bigtriangledown (h+z)\right|^{p-1} \bigtriangledown (h+z)$$

respectively. In this, *B* and B_s are flow parameters, *p* is Glen's flow law parameter, *N* is the normal stress due to the ice sheet, and *P* is the basal water pressure. Additionally, *z* refers to the topographic (bedrock) elevation, while *ρ* and *g* are the ice density and gravitational acceleration, respectively. Velocity is scaled using a scalar constriction factor, based on a second-order latitudinal ice surface gradient, $\frac{d^2z}{dx^2}$. In a simple scenario, u_d should be relevant where the basal ice temperature is below the melting temperatures, and u_d + u_s should be relevant where basal temperatures are above melting. This disregards the role basal hydrology may play, even at cold elevations, where melt water from warm days may percolate downward. Following Hubbard et al. (2005), the ice sheet is assumed to be isothermal and warm-based throughout.

Expanded mass balance

We obtain mass balance, M, by expanding it into accumulation and ablation calculations. Previous glacier models have typically computed mass balance as a single entity rather than splitting the calculation into a positive and a negative component (Hulton et al., 1994; Hubbard et al., 2005). The common approach is to define a mass balance curve that relates net change in mass at a point to elevation. The point in the curve at which $M = 0$ is the local ELA, which may be parameterized over the entire domain as an ELA surface. Computing M at any point on the map, then, is accomplished by solving a simple quadratic or cubic equation. A contrasting approach is used here. The advantage of expanding the calculation is that it allows us to separately consider the physical processes responsible for accumulation and ablation. An ELA and mass balance curve can then be retrieved from the result, rather than being defined as an input.

Accumulation is determined by applying a linear model to account for orographic precipitation, (Smith and Barstad, 2004). This treatment of orographic precipitation advects moisture over topography, calculating condensation and fallout based on physical conditions and time delays for condensation and free fall. Fourier transform methods are used to quickly calculate a precipitation field over realistic topography, yielding an estimate of precipitation that can be applied to the ice model with every time step. Using an orographic precipitation field distinguishes our approach from that of others, which have often used a mass balance curve to evenly accumulate mass based on elevation as shown by Hulton et al. (1994).

The precipitation predicted by the above theory is that which would fall under storm conditions. Realistic weather can be expected to be variable from month to month within the Patagonian climate. For this reason, the accumulation term is described as discrete moisture-delivering events over the course of the year, with each event having a characteristic duration. The hourly delivery is calculated from the linear theory, and then scaled for the year, given an annual frequency of events and event duration. The event frequency and duration are, in this case, not necessarily informed by data recording individual events, but instead by the accumulated annual precipitation. For efficiency, precipitation fields for a variety of seasons and conditions were not calculated and combined. Instead, the natural distribution in

storm conditions (wind direction and strength, season, etc.) is imitated by applying a background precipitation rate on top of the predicted field.

The drying of air as it moves over a region and condenses water is described here by a drying factor, *Df*. Application of a drying factor is necessary because the reduction in precipitation in downstream regions of the model domain is a nonlinear effect that is not included the linear precipitation model used. The Climatic Research Unit (CRU) makes available interpolated station records in the form of published 10' gridded data (New et al., 2002). These data are used to fit the drying factor, which is applied to the precipitation field by

$$M_{accum} = M_{lin} + \left(1 + \frac{\sum_{i=1}^{n} M_{lin} * Df}{\sum_{i=1}^{x} M_{lin}} \right)$$

where M_{lin} is the linear theory prediction, *n* is a point downwind on the model grid, and *x* is length of the model grid in a direction parallel to the wind vector. The effect of this equation is to simply remove a proportion from water from the precipitation field based on the potential amount of water that could fall from a saturated atmosphere, and the *Df*. Note that in this context the drying factor refers to the decrease in the amount of moisture that condenses and actually falls to the ground as precipitation, rather than to a measure of the actual change in the integrated vapor column in the atmosphere described by Smith and Barstad (2004).

Finally, the accumulation is determined by relating M_{accum} to the surface temperature, calculated from a lapse rate. Where the surface temperature is below the freezing temperature, precipitation is considered to be preserved.

Ablation is predicted on the basis of ambient temperature, calculated along a vertical lapse rate. Surface temperature is estimated based on surface topography (bedrock and ice thickness combined) and a typical lapse rate. For each model year, two surface temperatures are determined based on mean temperature records, with one corresponding to months September through March, and one to months April through August. For each half year, ablation is calculated separately. When temperature, T_s, is above

the melting point for ice, T_m, the ablation is predicted by multiplying the temperature difference by a degree-year factor f_m,

$$M_{ablate} = f_m(T_s - T_m)$$

for $T_s \geq T_m$, as suggested by Hock (2003). From this, it is clear that ablation is a linear function of temperature for temperatures above the melting point. Below the melting point, no ablation is predicted to occur. For f_m, I use the value reported by Braithwaite after conducting a 512-day study on the Nordboglacier in Greenland (1995).

The effect of dividing the year into two seasons is to improve the way in which the model deals with portions of the ice sheet near the freezing point. Summertime temperatures, rather than annual mean temperatures, dominate annual mass balance. If the annual mean temperature at a point were only a few degrees below the freezing point, ablation calculated by considering the year as a single unit would be zero. In reality, during much of the year, such as during summer months, ablation is likely occur. Modeling two seasons establishes a compromise that includes this effect to a first order, while limiting the increase in processing cost.

When accumulation and ablation are calculated separately, they can be added together to recover a mass balance curve and ELA, similar to those which are prescribed as a function in other models. By recovering the ELA as a dependent variable, we can compare the mass balance returned from this model to that which is used to describe climate change in other models. The ELA that evolves from our algorithm is analogous to the ELA that develops naturally in the field, rather than a model input. This gives us a better tool for comparing the solutions of our model to field measurement.

Complete model algorithm

ICE solves for ice thickness, velocity, and extent over a time-stepping finite difference grid. Based on topography, ICE calculates accumulation and ablation of the ice over a short time step. The model then computes the deformation and basal sliding of the accumulated ice over the grid, conserving mass and bedrock topography. The next model cycle begins, with more ice added or ablated based on the current environmental conditions (figure 4). After experimenting with different time step intervals, it was determined that a time step of roughly 1 month (0.1 years) provides a reasonable compromise between

computational efficiency and realistic ice flow through valleys. Because accumulation over large areas is relatively computationally-expensive to determine at every time step, yet sensitive to changing ice thickness and temperature, accumulation is recalculated on a 100 year interval. Ablation is also temperature-sensitive, but because it is inexpensive to apply the simple model outlined above, it may be recalculated on a more frequent basis.

Climate variables

The two independent variables that we manipulate are temperature and precipitation. The model has been tested using temperatures that either vary hypothetically as a sinusoidal function of time, or that are read from a script of prescribed temperatures, which can be based on paleotemperature proxies such as pollen or ice core isotope ratios. Likewise, precipitation can vary as defined by either an analytic function or a prescribed script.

Climatic parameters on which the model depends are constrained using CRU interpolated station data, published estimates of temperature depressions (Denton et al., 1999), and NCEP/NCAR reanalysis-based estimates of storm conditions (Smith and Evans, 2007). LGM simulations taking place over the past 125 ka are driven using temperature records derived from the Antarctic Vostok ice core data. In order to test the hypothesis that a shift in precipitation could account for a glaciations, additional model runs were completed with periodic variations in temperature over different time scales corresponding to a 40 ka glacial cycle, a 100 ka glacial cycle, and a hypothetical 200 ka glacial cycle. For a listing of physical and climate parameters used, see the appendix (table 1).

Results:

Many model runs have been conducted to test the ice sheet sensitivity to mean temperature, temperature range, and precipitation (storm frequency). Temperatures are reported in terms of the 10th and 90th percentile temperatures, because this gives a realistic impression of the effective temperature range over a long period, with short-term fluctuations have been filtered out. Precipitation is adjusted in terms of storm frequency, with constant storm intensity and length. Changes in precipitation are reported in terms of storm frequency, with the modern frequency pinned at 52 storms yr^{-1}. With the chosen storm

length and background precipitation rate, this gives annual precipitation totals comparable to what is available in climate data sets (New et al., 2002).

The LGM is used as a testing scenario to verify the model operation. This is possible because numerous field studies and other models have given us more information about the most recent of major glaciations than any other. It is possible to use this model to create an ice sheet with characteristics that fit what we know of the LGM ice sheet while keeping precipitation amount similar to what we know of present values. Ice sheet volume and extent are found to be extremely sensitive to temperature, such that large changes in the mean domain temperature are capable of rapidly generating major ice sheets in response. The modeled ice sheet that best fits the historical extents based on the above-described Last Glacial Maximum moraines is grown with a temperature depression of 7.4º Celsius, from the 10th and 90th percentile temperatures (figure 5). The mean modern ELA generated by the model varies spatially and is centered around 1400 m, while the LGM ELA ranges from 250-400 m. The ice sheet reaches a maximum volume at 25.9 ka, however the peak thickness occurs later, at about 22.9 ka. At its greatest extent, the ice sheet stretches over 129,000 km^2, while for comparison, the modern ice sheet extent is 9% of that of the returned LGM value, at 11,700 km^2.

The build-up of ice in this scenario is fairly quick, occurring at around 118 ka. From figures of the spatial distribution of ice (figure 6), it can be seen that the ice rapidly expands to reach the edge of the continental shelf to the west, where it is prevented from extending further by deep water. Once the extent of the ice covers much of the high topography (roughly 120,000 km^2) its growth levels off, but it continues to thicken. The large build-up of ice reduces the already limited supply of moisture to the west, and the slow growth of the ice sheet from this point on is primarily due to the eastward flow from the center of the topographic divide. As a part of this creeping growth, a tongue of ice over extends in the Balmaceda valley north of Lago Buenos Aires, surpassing mapped LGM limits. Another ice tongue fills the Lago Buenos Aires basin, and pushes outward. This ice tongue reaches a maximum length at about 16 ka corresponding well with the Fenix I and Fenix II moraines (Douglass, et al., 2006), after which it begins a slow retreat coincident with the rapid rise in temperatures. At about 11 ka, the entire ice sheet

experiences a catastrophic decline, lagging the decline in temperature by several thousand years (figure 7).

With the LGM conditions established, the response of the model to other conditions is explored. In contrast to the sensitivity to temperature, precipitation plays a smaller role. Minor changes in the storm frequency on the order of 10 storms yr^{-1} cause moderate increases in the ice cap size, but do not induce major glaciations of the order observed in the morainal record. Enormous increases, such as doubling the amount of precipitation to 104 storms a^{-1}, do cause major ice growth on the western side of the range. On the wet side of the range, the extremely large amount of ice accumulating at high elevations last long enough despite high ablation at low elevations to flow large distances westward. The build-up of significant topography in the form of an ice mountain influences in the orographic precipitation distribution, depositing more mass before and on top of the developed ice front. Despite the development of a large glacier system, no major ice tongues flow eastward on the opposite side of the topographic divide.

The plausibility of a precipitation-driven GPG is tested. The northward movement of the storm track may have been accompanied by some decrease in temperature. A small degree of temperature variation is permitted (a 3ºC depression incremented over 100 ka) and storm frequency is allowed to double in synchronization with temperature, a large ice sheet can be formed. This scenario is a rough hypothetical case in which the storm track presently at 56ºS is shifted northward to intersect the model domain. The ice sheet that results is primarily forced by dramatically increased precipitation, with only minor temperature forcing. The character of the precipitation-driven ice sheet is different from the entirely temperature-driven LGM ice sheet explored above. As with precipitation-only scenarios, the spatial distribution of the ice is more oriented toward the western side of the Cordilleran topographic divide, where moisture delivery is concentrated (figure 8). Ridges of ice can be seen to form along the Peninsula de Taitao, which then migrate westward by blocking subsequent snowfall on their eastern slopes. Much of the domain remains above melting temperature, so large lobes and curtains of ice pouring from high accumulation zones to lower elevations are rapidly ablate and often fail to move as far downstream as in the LGM case, where cooler low elevation temperatures ablate the ice more slowly. Significant eastward-

flowing lobes never form during model runs using any of the combinations of parameters tested. The implications of this result are discussed below.

Discussion:

The Last Glacial Maximum

The degree to which the modeled solution of the LGM ice sheet corroborates existing proxies for temperature in Patagonia gives credibility to its ability to simulate glaciations under conditions similar to those outlined above. The relatively straightforward modern precipitation distribution and good fit between calculated and observed precipitation fields help to make a realistic result attainable with simple model parameters. The modern ELA solution of 1400 m fits within estimates by others, which range from 700 m to 2000 m on different Patagonia glaciers (Hulton et al., 1994) and sits near 1500 m in the Northern Patagonian ice sheet (Broecker and Denton, 1990). The actual height of the ELA should change from west to east because of higher accumulation rates to the west, and higher continental summer temperatures to the east. The model output of LGM ELA depression is large compared to other estimates, which range from 350-1000 m. This value is sensitive mostly to seasonal parameters, particularly the summer temperatures that can be expected to vary widely across the real-world region.

The Greatest Patagonian Glaciation

Based on CRU data, the northern Patagonian ice sheet is within the northern limit of the wet Andes, where precipitation delivery is high. A fairly minor northward shift in the precipitation field, therefore, cannot alone explain the onset of a major glaciation. The modern storm track passes in the modern by the very southernmost tip of the South American Peninsula, at roughly 56ºS (Trenberth, 1991) A major shift (roughly 10º) could place the ice sheet directly on the path of the storm track, and intermediate changes may also cause higher precipitation. If it is possible that a steeper meridional temperature gradient during a global temperature depression could increase the frequency or intensity of storms, then a precipitation-driven ice sheet is feasible. The results of the modeled precipitation increase combined with a mild temperature depression support this conclusion, yet at the same time shed doubt on the hypothesis that such an ice sheet could have deposited the observed GPG Telken moraines.

The growth of a precipitation-driven ice sheet is based in the increased delivery of mass of a relatively small accumulation zone, rather than on an expansion of the accumulation zone as in the case of a temperature-driven ice sheet. Based on the model solutions, the mass delivery of a precipitation-driven ice sheet is concentrated more strongly on the weather side of a mountain range, and the smaller amount that blows over or falls from atypical storm events cannot over balance high ablation rates resulting from the higher average domain temperature. The growth of the ice-sheet is more strongly related to the location of the accumulation zones than with a temperature-driven ice sheet, in which there is more flow of ice from accumulation-dominated regions into lower elevations. The build-up of a high ridge of ice on the range exacerbates the east-west imbalance of ice mass by capturing more moisture, and blocking it more effectively from falling to the east. As a result, the ice sheet that grows fails to extend into valleys on the lee side of the range. In the region of study, the portion of the domain to the east of the topographic divide is too starved of moisture for accumulation to compete with ablation. An ice sheet that could have deposited the Telken VII moraine would, by necessity, have had to extend very far to the east. It is difficult to recreate the Greatest Patagonian Glaciation primarily by adjusting precipitation delivery, or without a temperature depression at least comparable to that determined for the LGM.

While fitting temperature depressions to the LGM Fenix moraines, it was noted that once a tongue of ice has filled most of the Lago Buenos Aires valley, only a small shift in temperature or increase in time at a low temperature can cause a large difference in the maximum extents of the glacier. This suggests that a GPG ice sheet could have been the result of temperature depressions similar to those that occurred during the LGM, or a combination of significant temperature depression and a precipitation increase.

Discussion of assumptions

An important simplification made in the physical properties of the ice is the assumption that ice is isothermal at the melting point, and for that reason, uniformly sliding. Hubbard et al. (2005) have defended that the decision to model the ice as isothermal is valid because there exists very little data from the Patagonian ice sheets to suggest otherwise. A large amount of heat would need to be removed from the glacier to convert all pore and interstitial water to ice, which will favor the isothermal condition. If evidence were available to suggest that the ice at high latitudes is or has been frozen-based it would imply

a generally thicker ice sheet with lower velocities at high elevations. At lower elevations, such as in the vicinity of the terminal moraines, the ice is more likely to be warm-based, even during a deep glaciation. Although the distinction between frozen and warm-based ice at high elevations will indirectly affect the movement of downstream ice, the warmer low elevation temperatures will limit the direct effects of this assumption.

In contrast to the ice deformation and accumulation, the ablation model is more simplistic. There is no mechanism built into the model to allow the attitude of topographical slopes to influence melting, and there is no transport of heat or mass by meltwater runoff. The parameters that play a role in ablation are poorly known. Because there are limited direct observations of ablation distribution across the modern ice sheet (Takeuchi, 1996), there is no clear way to independently test the way in which ablation is calculated. The data used to inform the degree-year factor are derived from a dry continental ice cap, which may not be translatable to the modern temperate glaciers. That changing climatology and atmosphere over the ice during the LGM may make the Greenland data more applicable, but this is speculation.

Division of the year into two seasons is a coarse approximation that does not necessarily capture the effect of one or two summer months of peak temperature, or conversely, a couple winter months of intense cold. Also, as mentioned above, the seasonal variation over the course of a year is approximated to be constant for simplicity. Because ice mass is very sensitive to summer temperature, differences in seasonal temperature change can play an important role in overall mass balance, and will have an effect on the estimated temperature and ELA depressions required for a major glaciation.

Perhaps the most critical simplifications are the level temperature plane and the constant lapse rate, which together mean that all points on a plane of constant elevation have the same temperature. This means that the only influence continentality has on the model is the gradual drying of the atmosphere to the east. A more nuanced temperature model would capture the observed higher and lower temperature extremes that occur east of the range, which will influence the temperature forcing required to generate an ice sheet.

Summary:

A coupled orographic precipitation model and ice-routing model has been applied to ice sheet evolution in the Patagonian Andes. Rather than model climate changes with shifts in a prescribed ELA, the model makes it possible to consider changes in physical conditions directly. Based on the glacial extents inferred from depositional features, a climatic forcing to drive the model has been estimated using Vostok ice core data as a constraint for temperature. Assuming modern storm frequency to have existed over the past 100 ka, then the LGM glaciation in the vicinity of Lago Buenos Aires can be recreated with a temperature depression of 7.4º Celsius, which is in good agreement with other estimates. The modern ELA has been retrieved from the model. Glacial ELA depressions determined from the model are large, but improved descriptions of ablation could modify this estimate. This model is used to test the sensitivity of the Patagonian ice sheet to elevated levels of precipitation delivered by mid-latitude storms. If storm frequency is increased, the temperature changes required to depress the ELA become more modest, however increasing moisture delivery has a stronger effect on ice volume on the western half of the topographic divide. Because of this, it does not appear to be feasible to argue that the extensive GPG was driven primarily by an increase in storm frequency, without a simultaneous lowering of summer temperatures. Because large mountain ranges such as the Andes effectively dry the atmosphere as it passes across them, it is difficult to build or maintain an ice sheet under high ablation conditions on the eastern side of the Andes.

Both precipitation and temperature have the potential to be limited factors in the development of an ice sheet, but under the environmental conditions at the northern Patagonian ice field, temperature dominates. Because of the important role temperature is demonstrated to play, further work on modeling the area should focus on refining the temperature field and ablation calculations.

Acknowledgments:

I would like to express my gratitude for guidance, advice, and constructive criticism received from Mark Brandon, Ron Smith, Frederic Herman, Keith Laskowski, and Ric Wilson. Interest in the subject was sparked with help and encouragement from Mark Brandon, Stuart Thompson, and Peter Reiners.

References Cited:

Anderson, R. S. (2008). Departmental colloquium presentation. Yale University.

Casassa, G. (1987). Ice thickness deduced from gravity anomalies on Soler Glacier, Nef Glacier, and the Northern Patagonia Icefield. *Bulletin of Glacier Research*, 4, 43-57.

Caldenius, C. C. (1932). Las glaciaciones cuaternarias en la Patagonia y Tierra del Fuego. *Geografiska Annaler*, 14, 1-164.

Broecker, W. S., and G. H. Denton (1990). The role of ocean-atmosphere reorganizations in glacial cycles. *Quaternary Science Reviews*, 9, 305-341.

Denton, G. H., C. J. Heusser, T. V. Lowell, P. I. Moreno, B. G. Andersen, L. E. Heusser, C. Schlüchter, and D. R. Marchant (1999). Interhemispheric linkage of paleoclimate during the last glaciation. *Geografiska Annaler*, 81 A, 107-153.

Douglass, D. C., B. S. Singer, M. R. Kaplan, R. P. Ackert, D. M Mickelson, M. W. Caffee (2005). Evidence of early Holocene glacial advances in southern South America from cosmogenic surface-exposure dating. *Geology*, 33, no. 3, 237-240.

Douglass, D. C., B. S. Singer, M. R. Kaplan, D. M Mickelson, M. W. Caffee (2006). Cosmogenic nuclide surface exposure dating of boulders in last-glacial and late-glacial moraines, Lago Buenos Aires, Argentina: Interpretive strategies and paleoclimate implications. *Quaternary Geology*, 1, 43-58.

Hartmann, D. L. (1994). *Global physical climatology*. New York: Academic Press.

Herman, F., and J. Braun (2008). Evolution of the glacial landscape of the Southern Alps of New Zealand: Insights from a glacial erosion model. *Journal of Geophysical Research*, 113, F02009.

Hock, R. (2003). Temperature index melt modelling in mountainous areas. *Journal of Hydrology*, 282, 104-115.

Hubbard, A., A.S. Hein, M.R. Kaplan, N.J. Hulton, and N. Glasser (2005). A modelling reconstructions of the Last Glacial Maximum ice sheet and its deglaciation in the vicinity of the Northern Patagonian Icefield, South America. *Geografiska Annaler*, 87A, 375-391.

Hulton, N. R., D. Sugden, A. Payne, and C. Clapperton (1994). Glacier modeling and the climate of Patagonia during the Last Glacial Maximum. *Quaternary Research*, 42, 1-19.

Hulton, N. R., R. S. Purves, R. D. McCulloch, D. E. Sugden, and M. J. Bentley (2002). The Last Glacial Maximum and deglaciation in southern South America. *Quaternary Science Reviews*, 21, 233-241.

Kaplan, M. R., D. C. Douglass, B. S. Singer, R. P. Ackert, and M. W. Caffee (2004). Cosmogenic nuclide chronology of pre-last glacial maximum moraines at Lago Buenos Aires, 46ºS, Argentina. *Quaternary Research*, 63, 301-315.

Kaplan, M. R., A. S. Hein, A. Hubbard, and S. M. Lax (2009). Can erosion limit the extent of glaciation? *Geomorphology*, 103, 172-179.

Mercer, J. H. (1983). Cenozoic glaciation in the southern hemisphere. *Annual Review of Earth and Planetary Sciences,* 11, 99-132.

Murdie, R.E., D. T. Pugh, and P. Styles (1999). A lightweight, portable, digital probe for measuring the thermal gradient in shallow water sediments, with examples from Patagonia. *Geo-Marine Letters*, 18, 315–320

New, M., D. Lister, M. Hume, and I, Makin (2002). A high-resolution data set of surface climate over global land areas. *Climate Research*, 21, 1-25.

Singer, B. S., L. L. Brown, J. O. Rabassa, and H. Guillou (2004). $^{40}Ar/^{39}Ar$ chronology of Late Pliocene and Early Pleistocene geomagnetic and glacial events in southern Argentina. *Geological Society of America Bulletin*, 116, no. ¾, 434-450.

Smith, R.S., and I. Barstad (2004). A linear theory of orographic precipitation. *American Meteorological Society*, 61, 1377-1391.

Smith, R.S., and J.P. Evans (2007). Orographic precipitation and water vapor fractionation over the Southern Andes. *Journal of Hydrometeorology*, 8, 3-19.

Takeuchi, Y., R. Naruse, P. Skvarca (1996). Annual air-temperature measurement and ablation estimate at Moreno Glacier, Patagonia. *Bulletin of Glacier Research*, 14, 23-28.

Thompson, S. N., M. T. Brandon, P. W. Reiners, J. H. Tomkin, C. Vásquez, N. J. Wilson. A poleward transition from constructive to destructive glacio-climatic control on mountain building. In prep. Presented at AGU Fall Meeting, 2007, C41A-0051.

Trenberth, K. E. (1991). Storm track in the southern hemisphere. *Journal of the Atmospheric Sciences.*, 48, no. 19, 2150-2178.

Figures and Appendices:

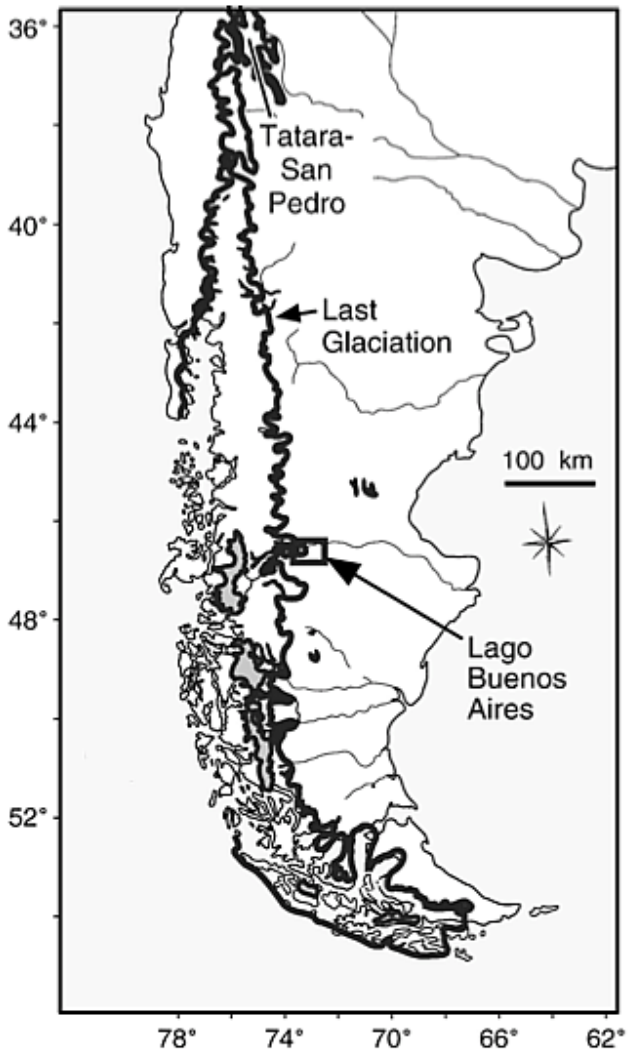

(Figure 1) Overview of the Last Glacial Maximum icesheet extents, with the Lago Buenos Aires model area indicated near 47ºS latitude. Moving south from the northern edge of the ice sheet, the western ice margin moves farther west, eventually moving offshore. The eastern extent stays more constant, but pushes out where flowing ice converges into drainages, becoming thicker. The Lago Buenos Aires valley is one example of where ice from the interior of the range has converged had left far-reaching eastern terminal moraines. Image from Kaplan (2004), with data from Caldenius (1932).

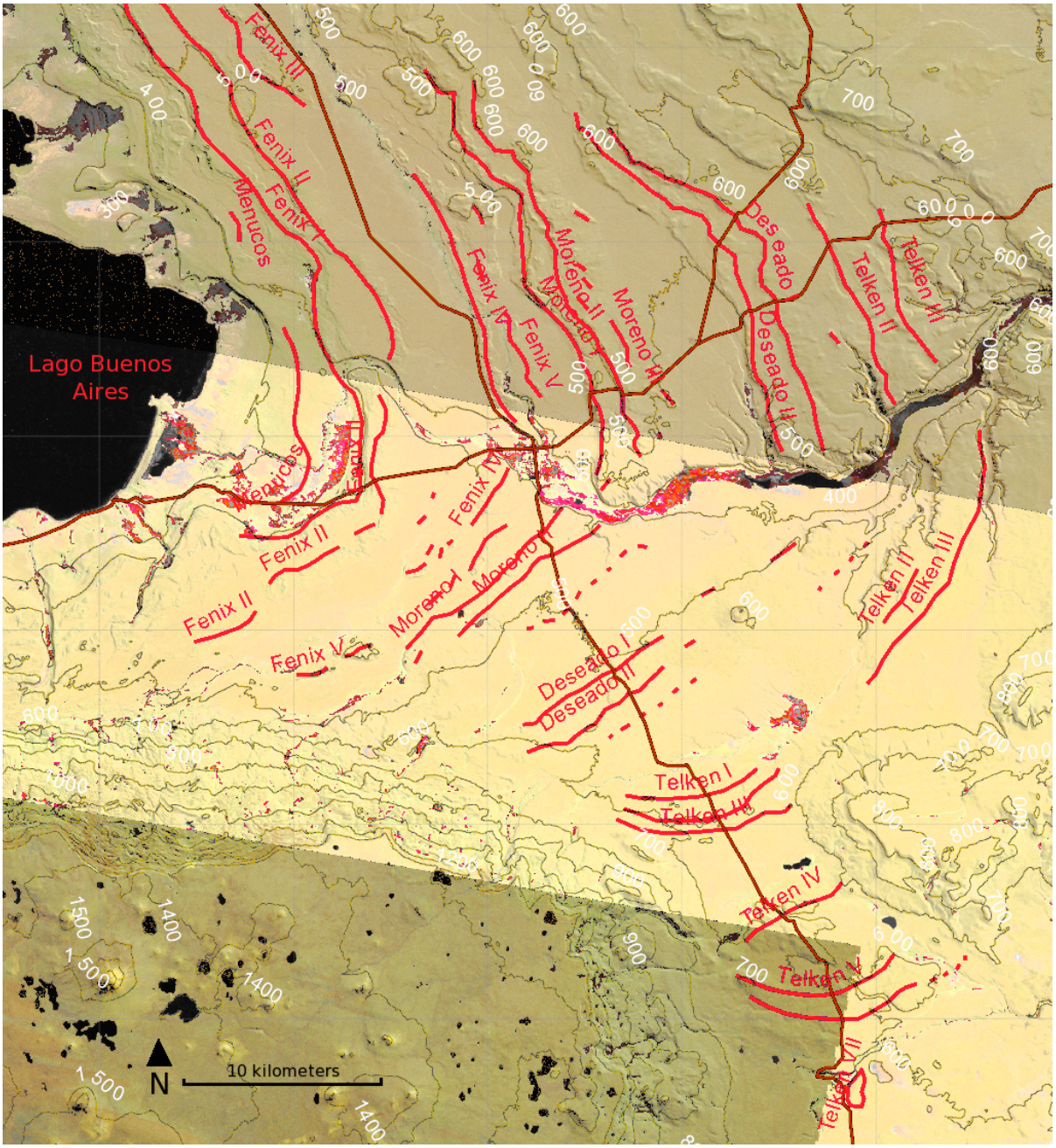

(Figure 2) Locations of moraines deposited by successive Lago Buenos Aires glaciations between 1 Ma and the present. The LGM Menucos and Fenix moraines are visible in northwest, near the modern lake shoreline. The GPG Telken VII moraine is accessible from the road in the southeastern corner. Data from Kaplan (2004); figure provided by Keith Laskowski.

(Figure 3) Lago Buenos Aires "mask" used with recorded soundings (Murdie, et al, 1999) to generate synthetic bathymetry for the digital elevation model.

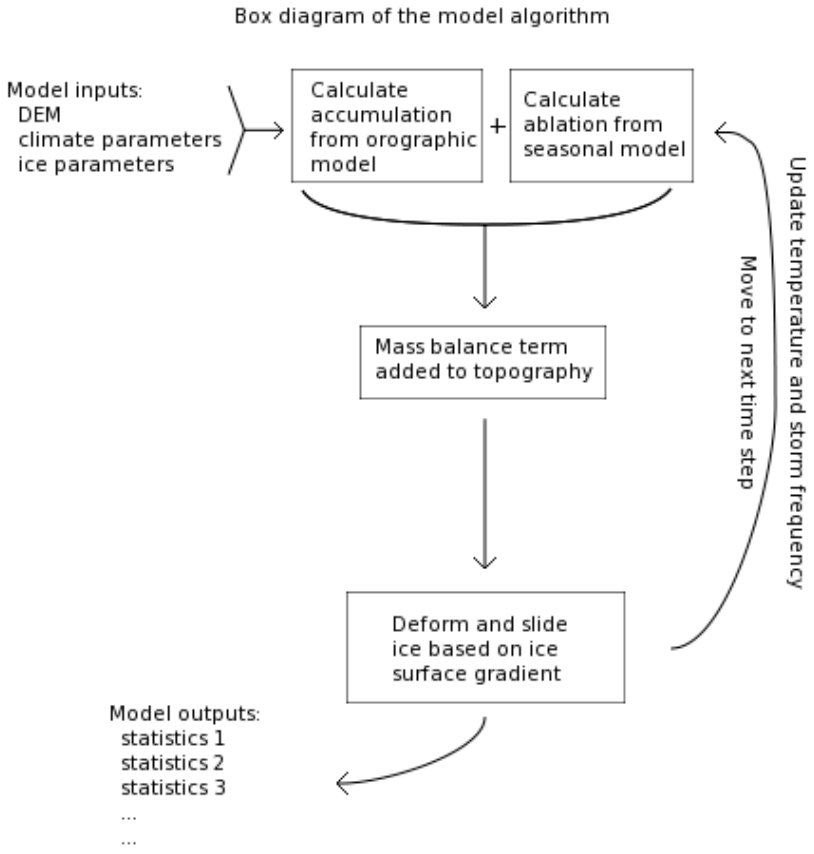

(Figure 4) Schematic diagram of the model algorithm. Inputs are the DEM, climate parameters used to define precipitation and temperature fields, and the ice flow parameters. The orographic precipitation is used to determine accumulation, and the temperature field is used to determine ablation, which are combined into a mass balance term. This creates an initial ice thickness, which can change based on the ice rheology. The model is recursive, continually iterating time steps until a predefined end moment.

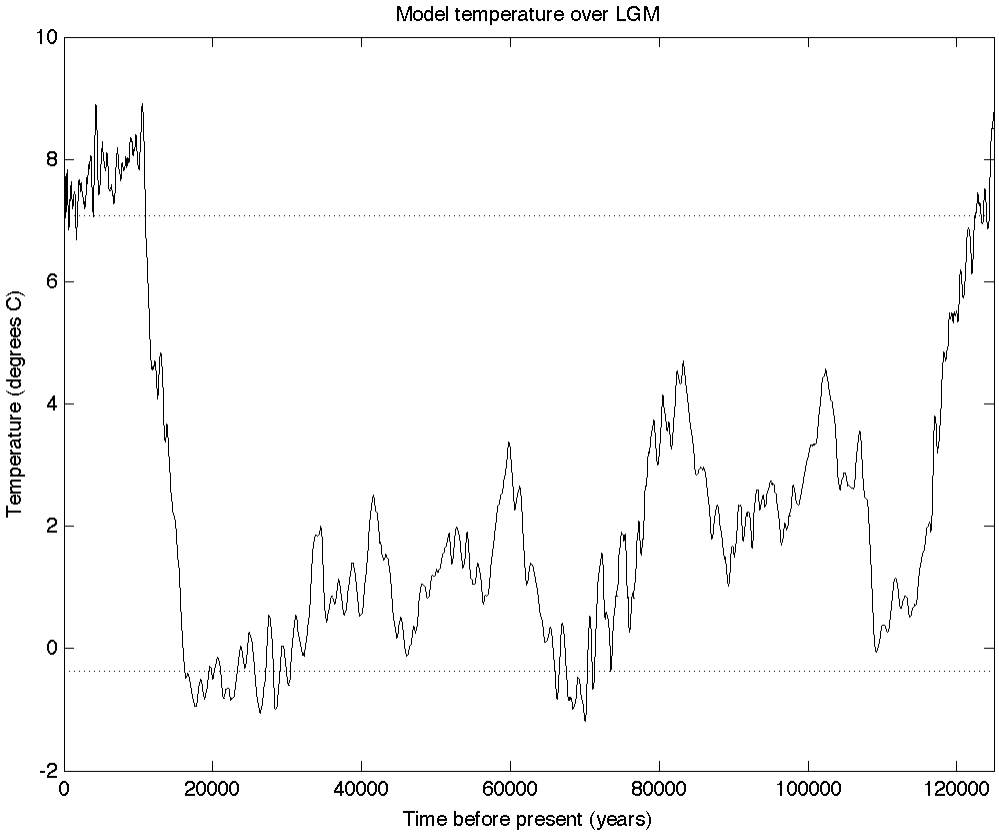

(Figure 5) Temperature data derived from the Vostok ice core was used to drive the model. The data was transformed and scaled to fit modern conditions as a boundary condition. Afterwards, the model was used to fit the data based on known ice extents. The dotted lines indicate the P10 and P90 temperatures, which are used as a measure of temperature range.

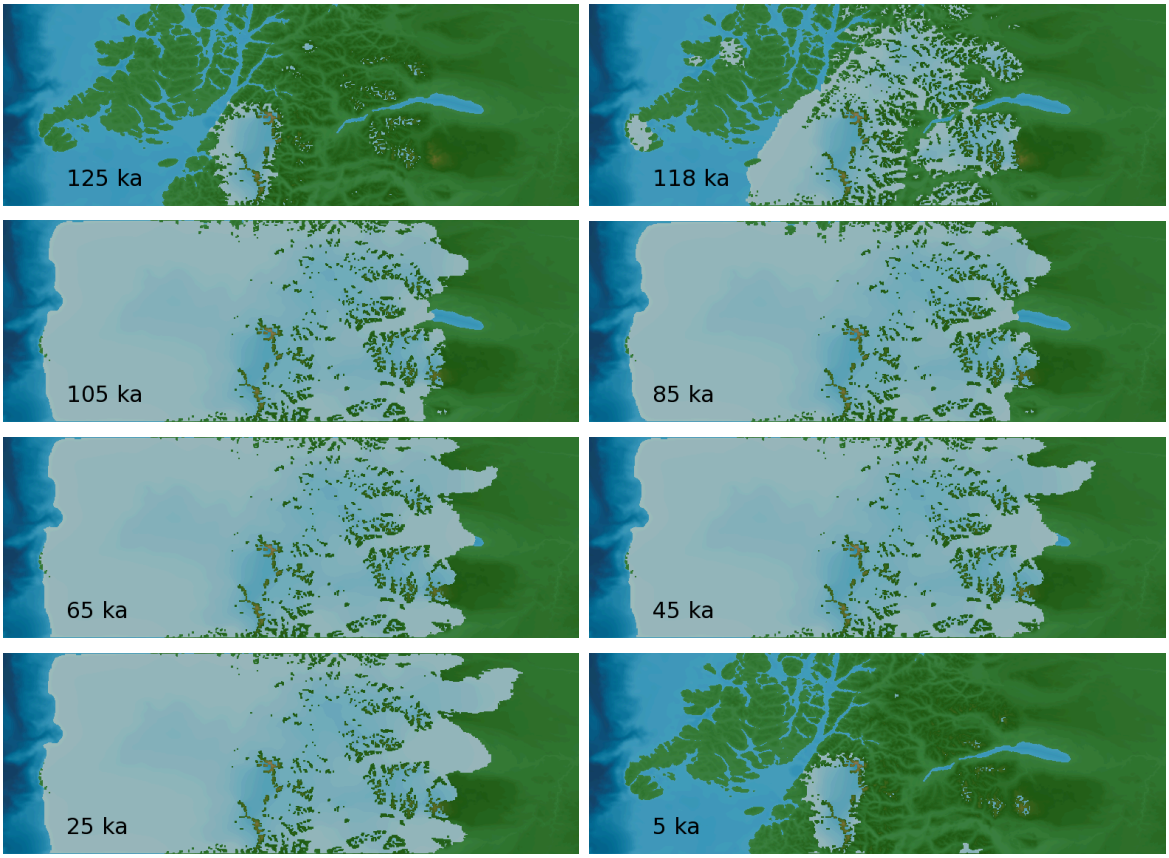

(Figure 6) Series of model snapshots from the best LGM simulation. Numbers indicate time relative to present. The model begins at 125 ka with a small ice cap similar to the modern ice cap. A rapid temperature drop (see figure 4) causes the ice sheet to expand, covering much of the range by 105 ka. Although the Lago Buenos Aires valley is generally below the equilibrium line altitude, flow of ice from higher elevations gradually pushes a tongue of ice down the lake, until it reaches the approximate location of the LGM Fenix moraine sequence. Large net ablation begins around 12 ka, and rapidly restores the ice cap to its pre-glaciation size.

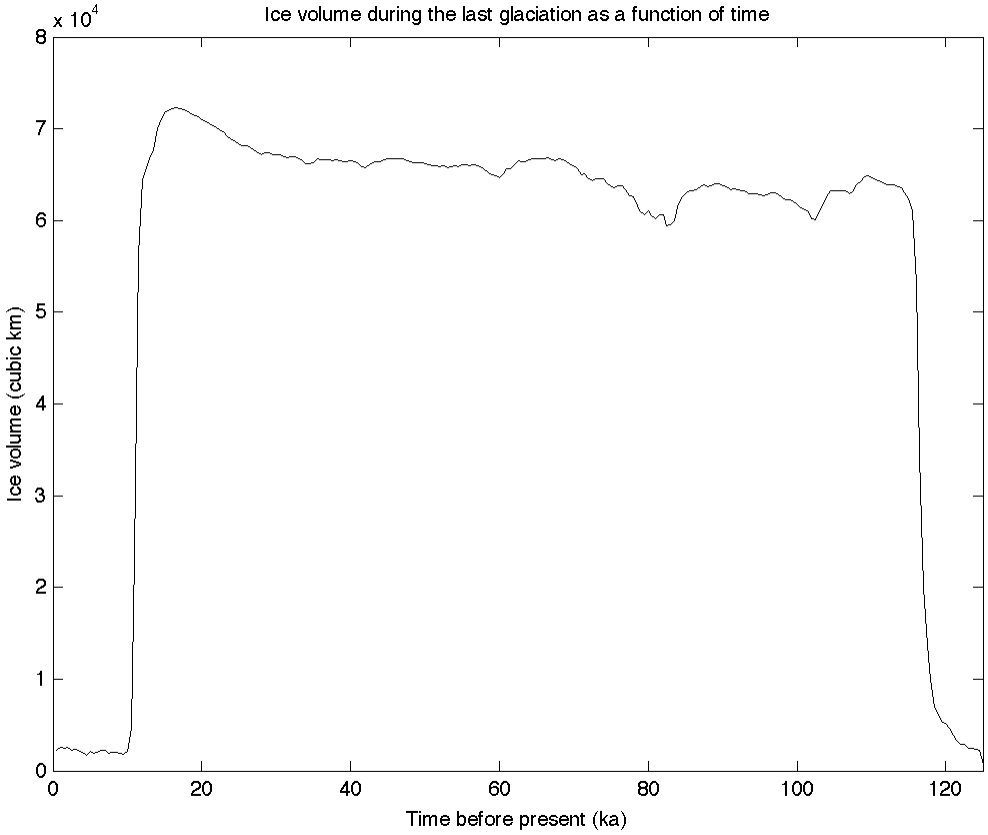

(Figure 7) Ice growth occurs rapidly from about 117 ka to 118 ka, before leveling off when the western portion of the domain is ice saturated to the continental shelf. Rapid decline begins around 12 ka, and is complete by 10 ka. Comparison with the temperature record demonstrates an insensitivity to minor fluctuations, with rapid transitions between glacial and interglacial climates once unstable.

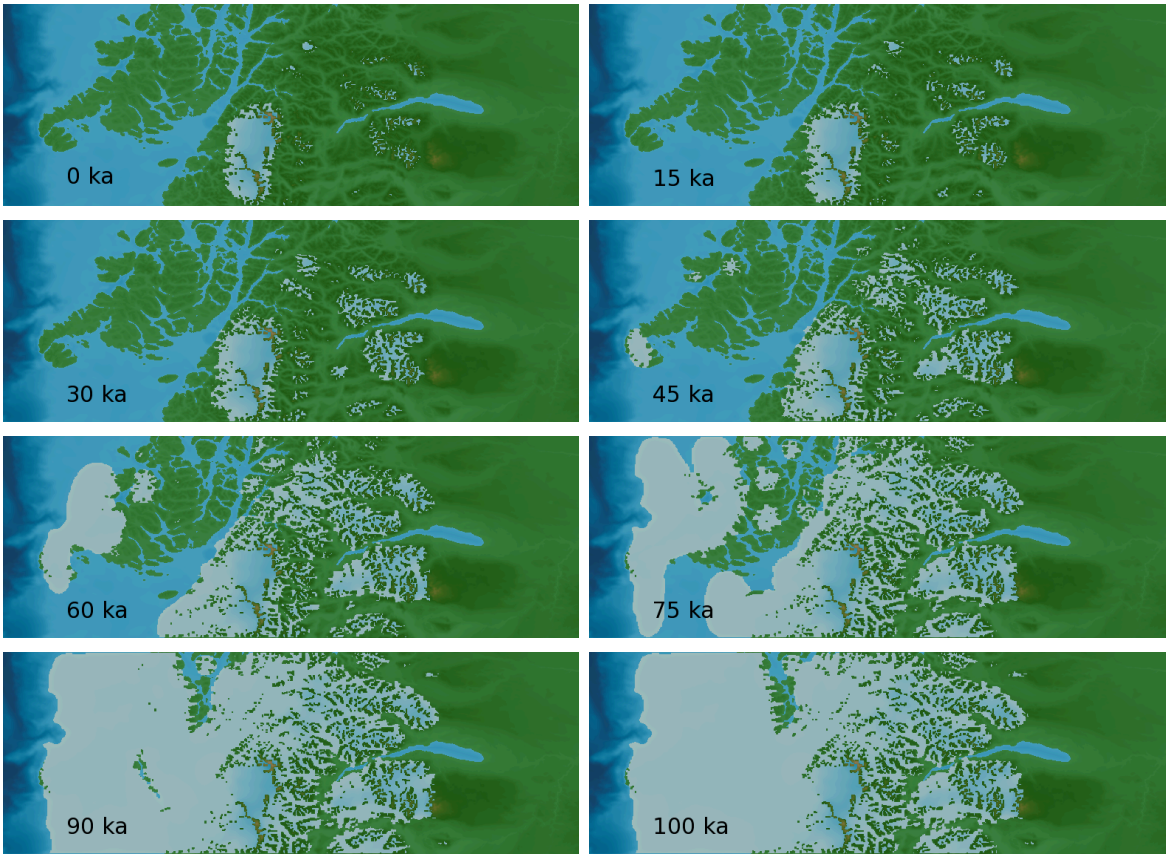

(Figure 8) Scenario in which precipitation and temperature both vary sinusoidally with a period of 200 ka. In this hypothetical scenario, numbers indicate time since model start. The starting condition is an ice sheet with extents similar to the modern. At 100 ka, temperature is depressed 3ºC, and storm frequency is double the modern value. A westward-growing ice sheet is formed, but no eastern ice sheet comparable to GPG (or even LGM) moraines ever forms. The Lago Buenos Aires basin remains ice-free, even when the western ice margin reaches the continental shelf.

(Table 1)

Model Framework Parameters:

domain extents	47.3ºS, 46.0ºS, 74.0ºW, 70.3ºW
grid spacing	925 m x 925 m
time step	0.1 a (100 a for mass balance recalculation)

Ice Flow Parameters:

Deformation constant, B	6.8×10^{-24} s^{-1} Pa^{-3}
Sliding constant, B_s	1.0×10^{-14} s^{-1} Pa^{-3} m^{-2}
Glenn's flow parameter, p	3
Ice density, ρ	910 km m^{-3}
Gravitational acceleration, g	9.81 m s^{-2}

Climate Parameters (LGM):

P90 temperature	7.07ºC
P10 temperature	-0.37ºC
Drying factor, *Df*	1.3
Atmospheric lapse rate, Γ	6.5×10^{-3} K m^{-1}
Zonal wind, u	11 m s^{-1}
Meridional wind, v	0.0 m s^{-1}
Condensation delay, τ_c	1300 s
Fallout delay, τ_f	2700 s
Background rate	5.6×10^{-7} m s^{-1}
Moist stability frequency	.0067 s^{-1}
Storm frequency scaling	52 a^{-1}
Storm length scaling	40 hr
Degree-year factor	3.0 m K^{-1} a^{-1}
Model time	125 ka

Climate Parameters (GPG):

Same as LGM model runs, except where noted. Temperature and storm frequency vary sinusoidally.

P90 temperature	6.93ºC
P10 temperature	4.07ºC
Storm frequency scaling	from 52 to 104 a^{-1}
Storm length scaling	40 hr
Degree-year factor	3.0 m K^{-1} a^{-1}
Model time	40 ka, 100 ka, 200 ka